

## Low-Frequency Noise Observed in the Distant Magnetosphere with OGO 1

N. DUNCKEL, B. FICKLIN,<sup>1</sup> L. RORDEN,<sup>2</sup> AND R. A. HELLIWELL

*Radioscience Laboratory, Stanford University, Stanford, California 94305*

Two new types of low-frequency noise, designated 'broadband' and 'highpass,' have been detected in the distant magnetosphere by the VLF/LF experiment on the OGO 1 satellite. Broadband noise extends over the entire range of observations from 0.2 to 100 kHz and the intensity decreases with increasing frequency. It occurs in bursts having durations of a few minutes or less. It shows no connection with any of the expected plasma cutoff or resonance frequencies and is believed to be a nonpropagating disturbance generated in the vicinity of the satellite. Highpass noise extends from a characteristic low-frequency cutoff to above 100 kHz and occurs in bursts lasting tens of minutes. This cutoff has only been observed above 20 kHz. Above the cutoff the intensity shows little variation with frequency. Both types of noise are observed predominantly at  $L$  greater than 5 in or near the night hemisphere. The occurrence of both types of noise is highly correlated with the auroral electrojet index. Several times noise bursts began within 2 min of the onset of micropulsations in the polar region even though the satellite was near apogee (24 earth radii). The peak rms magnetic intensity in a highpass noise burst has a maximum of  $8 \times 10^{-8} \gamma \text{ Hz}^{1/2}$  and averages  $10^{-8} \gamma \text{ Hz}^{-1/2}$ . In free space these magnetic intensities correspond, respectively, to  $10^{-19}$  and  $3 \times 10^{-14}$  watt  $\text{m}^{-2} \text{ Hz}^{-1}$ . The peak levels of both types of noise are 3 or more orders of magnitude stronger than emissions from extraterrestrial sources observed with interplanetary probes.

### INTRODUCTION

The OGO 1 satellite provided the first observations at geocentric distances from 2 to 24 earth radii of noise in the frequency range 0.2 to 100 kHz. From these observations two hitherto unreported noise phenomena were discovered at  $L > 5$  in or near the nightside of the earth. The intensity of these noises is considerably greater than that of cosmic, solar, or Jupiter noise observed at low frequencies in interplanetary space. Consequently these noises are likely to affect low-frequency radioastronomy and radio propagation experiments operating in the magnetosphere.

In addition to the two noise phenomena discussed here, the OGO 1 satellite has also observed whistlers with spectral components as high as 80 kHz, signals from ground-based transmitters [Heyborne, 1966] at various frequencies up to 100 kHz, and whistler-mode emissions up

to 50 kHz [Dunckel and Helliwell, 1969]. These types of noise, all of which occur below the local gyrofrequency, are easily differentiated from highpass and broadband noise by both their spectrum and occurrence, and will not be discussed further here.

The noises described here differ from the disturbances generally observed in radioastronomy experiments. Such experiments have measured electric field intensities well above the cosmic background level in the topside ionosphere (see review article by Haddock [1966]). These enhancements are generally restricted to frequencies below the upper-hybrid frequency  $f_{UH}^2 = f_p^2 + f_H^2$ , where  $f_p$  and  $f_H$  are the electron plasma and gyrofrequencies, respectively [Harvey, 1965, 1968; Huguenin and Papagiannis, 1965; Hartz, 1967, 1969]. In this respect these enhancements differ from broadband and highpass noises, which include components above the probable upper-hybrid frequency. In the distant magnetosphere, however, noise bursts that may be similar to those reported here have been observed above the probable  $f_{UH}$  in two radioastronomy experiments that measured electric fields at frequencies between 30 and 1525 kHz [Benediktov et al., 1966; Slysh, 1967a]. Accord-

<sup>1</sup> Stanford Research Institute, Menlo Park, California 94025.

<sup>2</sup> Develco, Inc., Mountain View, California 94040.

ing to Benediktov et al., emission intensities are correlated with fluxes of electrons having energies greater than 100 ev.

In interplanetary space the intensities in watts per square meter per Hertz observed from extraterrestrial sources are  $7 \times 10^{-37}$  at 30 kHz in a noise burst from Jupiter [Slysh, 1966]; as high as  $2 \times 10^{-36}$  at 200 kHz in a noise burst from the sun [Slysh, 1967b]; and a cosmic background level of  $6 \times 10^{-36}$  at 725 kHz [Benediktov et al., 1966]. These levels are near or below the threshold levels of the receivers employed here. One noise event of intensity  $\geq 10^{-36}$  watts  $m^{-2}$   $Hz^{-1}$  at 30 kHz was observed from the nightside of the moon; however, it is not clear that this event was of direct solar origin [Slysh, 1967b]. With this one possible exception, the radiation observed from extraterrestrial sources is several orders of magnitude too weak to account for the noise events reported in this paper. This conclusion is supported by the localized occurrence of these events on the night side of the earth and the nearly simultaneous occurrence of polar disturbance phenomena observed on the ground.

#### THE EXPERIMENT

The experiment that detected these phenomena has been described by Dunckel and Helliwell [1969]. It consists of a loop antenna of 2.9 meters diameter driving four receivers. The direction of maximum sensitivity of the loop antenna is essentially unchanged during the 12-sec rotation period of the satellite.

Three of these receivers sweep the ranges 0.2–1.6, 1.6–12, and 12–100 kHz with 3 db bandwidths of 40, 160, and 600 Hz, respectively. The background noise level varies from approximately  $2 \times 10^{-36}$   $\gamma$  rms at 0.3 kHz to  $6 \times 10^{-36}$   $\gamma$  rms at 100 kHz, which in free space is equivalent to  $2 \times 10^{-31}$  to  $10^{-37}$  watt  $m^{-2}$   $Hz^{-1}$ , respectively. A complete sweep from all three sweeping receivers is obtained once each 2.3, 18.4, or 147 sec, depending on the rate of data transmission from the satellite. The fourth receiver, designated the broadband receiver, provides the waveform and amplitude of signals in the 0.3–12 kHz range from which high-resolution spectra can be made on the ground.

The digitized outputs of the sweeping receivers are recorded on 16-mm film so that each frame on the film displays one sweep from

each sweeping receiver, as is demonstrated by the two consecutive frames of Figure 1. The vertical axes of each of the three graphs within a frame represent the magnetic intensity of a discrete-frequency signal in decibels below 1  $\gamma$ , and the horizontal axes represent frequency in kHz from 0.2 to 1.6 (top), 1.6 to 12 (middle), and 12 to 100 (bottom). The intersections of a vertical line with the three graphs mark data recorded essentially simultaneously. Possible telemetry errors are indicated by deviations from the line below the 12- to 100-kHz frequency scale (these appear near 37 and 50 kHz below the third graph of the upper frame). The background level, determined by the receiver noise plus spacecraft inverter interference at 0.4 kHz, 2.461 kHz, and their harmonics, has been derived from quiet data and is approximated by the light dashed line. Because of the close spacing of the inverter harmonics in the output of the 12- to 100-kHz receiver, we will call the background level in this frequency range the line connecting local minima. (In Figure 2 the spectrum between 0.2 and 45 kHz represents essentially background level.)

Data from the sweeping receivers exhibit interference from the radio beacon experiment [Fritz et al., 1968]. The interference was most noticeable just after this experiment was turned on; hence its identity was easily confirmed from the list of commands to the satellite. At frequencies above 2 kHz the effect of the interference was to raise the background level by about 10 db. Since the intensity of the phenomena discussed here is of the order of 30 db above the background level, it is doubtful that the interference affects in any way the conclusions reached here.

#### BROADBAND NOISE

Broadband noise is the name given to the phenomenon displaying a continuum of noise over the entire frequency range of observation (0.3–100 kHz). Figure 1 shows two consecutive frames of data from the nightside magnetosphere displaying this class of noise. As is typical for broadband noise, no inflection in the spectrum occurs near  $f_H = 3.1$  kHz. The marked fluctuations in the outputs of each of the three receivers are well correlated, indicating that what is being observed is not primarily a spectral variation but rather a temporal or

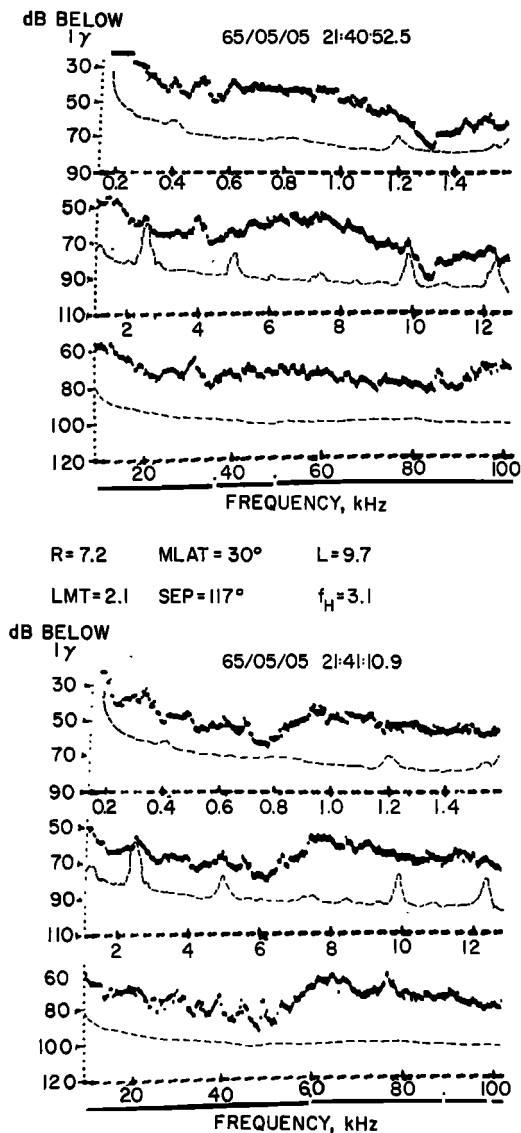


Fig. 1. Two consecutive frames demonstrating broadband noise in the outputs from the three sweeping receivers. The  $x$  axes are calibrated in kilohertz and the  $y$  axes in decibels below  $1 \gamma$  rms (i.e., 20 db represents  $0.1 \gamma$ ). Above each frame appears the starting time as year/month/day, hour:minute:second. Satellite location appears in terms of  $R$ , geocentric distance in earth radii;  $MLAT$ , magnetic latitude;  $L$  in earth radii;  $LMT$ , local mean time;  $SEP$ , sun-earth-probe angle; and  $f_H$ , the local electron gyrofrequency in kilohertz based on a simple dipole model. Approximate background levels are shown as dashed lines in each frame. Note wide spectrum of broadband event (0.2 to 100 kHz) and the rapid time variations that appear to be

spatial variation occurring over the 18.4 sec required to complete one frame. Some intensity variations are seen to occur in less than 1 sec. Since the mean duration of events similar to that of Figure 1 is approximately 7 minutes, they are often referred to as 'bursts.'

The intensity variation of broadband noise sometimes shows a well-defined component at the spin period of the satellite. In Figure 1, intensity minima at the right-hand side of the upper frame and at the middle of the lower frame are spaced in time by 12 sec, approximately the rotation period of the satellite. Spin modulation has not been seen on any other type of noise, nor was it expected, since the orientation of the axis of the loop, and hence its directional pattern, is virtually independent of spacecraft rotation. This indicates that broadband noise is in some way connected with the position in inertial coordinates of the antenna with respect to the spacecraft body and hence is of local origin.

The apparent intensity of the broadband noise in Figure 1 is well above the background level of the receivers. The median magnetic spectral density in  $\gamma \text{ Hz}^{-1/2}$  for the two frames of Figure 1 and three adjacent frames decreases from  $4 \times 10^{-8}$  at 0.3 kHz to  $8 \times 10^{-8}$  at 100 kHz. In these five frames the spectral density was approximately proportional to (frequency) $^{-1.7}$  in the range 0.3 to 2.4 kHz and to (frequency) $^{-0.5}$  in the range 12–100 kHz.

#### HIGHPASS NOISE

Highpass noise is characterized by a spectrum that is generally continuous from a frequency above the upper limit of the receivers (100 kHz) down to a low-frequency cutoff that may vary from frame to frame but has not yet been observed below 20 kHz. Figure 2 shows two consecutive frames of data in which the highpass noise displays a low-frequency cutoff near 45 kHz in the third graph. Below this frequency, the traces represent essentially threshold level (except for the small enhancements at 0.5 and 4.0 kHz seen in the lower frame, possibly caused by a broadband noise event whose

well-correlated in each receiver (i.e., sharp rise near middle of lower frame). The time required to complete each frame was 18.4 sec.

duration was very brief compared to the duration of the frame).

The variation in intensity of the highpass noise is generally less rapid than that for the broadband noise. The difference is illustrated by the consistency of the intensity of highpass noise from the upper to the lower frame of Figure 2 compared to the gross variations in broadband noise between the two frames of Figure 1. The spin modulation sometimes observed in broadband noise has not been detected in highpass noise.

The low-frequency cutoff is defined as the frequency at which the lower end of the emission spectrum coincides with the receiver background level. This cutoff can be seen to decrease slightly from the first to the second frame of Figure 2. Sequential frames show that the cutoff of a highpass noise burst often commences at a high frequency, descends to a minimum, and then rises before the burst ends. The cutoff is likely to be most sharply defined near this minimum frequency. This minimum varies relatively slowly with satellite position. In one case when its variation was particularly well defined, the minimum cutoff was observed to decrease from 90 kHz at a geocentric distance of 3.9 earth radii to 40 kHz at 5.4 earth radii. In this example the magnetic latitude and local mean time remained approximately constant at 34° and 23 hours, respectively. Thereafter the noise grew weaker and more sporadic, but the lower cutoff frequency remained approximately constant.

Above the cutoff the intensity is relatively independent of frequency. Small variations, such as the maxima near 60 and 100 kHz in Figure 2, are occasionally observed, however.

Although the temporal variations of highpass noise tend to be slower than those of broadband noise, intensity variations of 10 db have been observed while the satellite moved as little as 1/4 of the free-space wavelength at 100 kHz. Since spatial variations over this small distance are unlikely, this variation is probably temporal. It is therefore likely that longer-period variations are also temporal in origin.

From the OGO-1 data recorded from September 1964 through May 1965, 178 bursts of highpass noise have been identified. A burst is defined as a set of consecutive frames showing highpass noise preceded and followed by

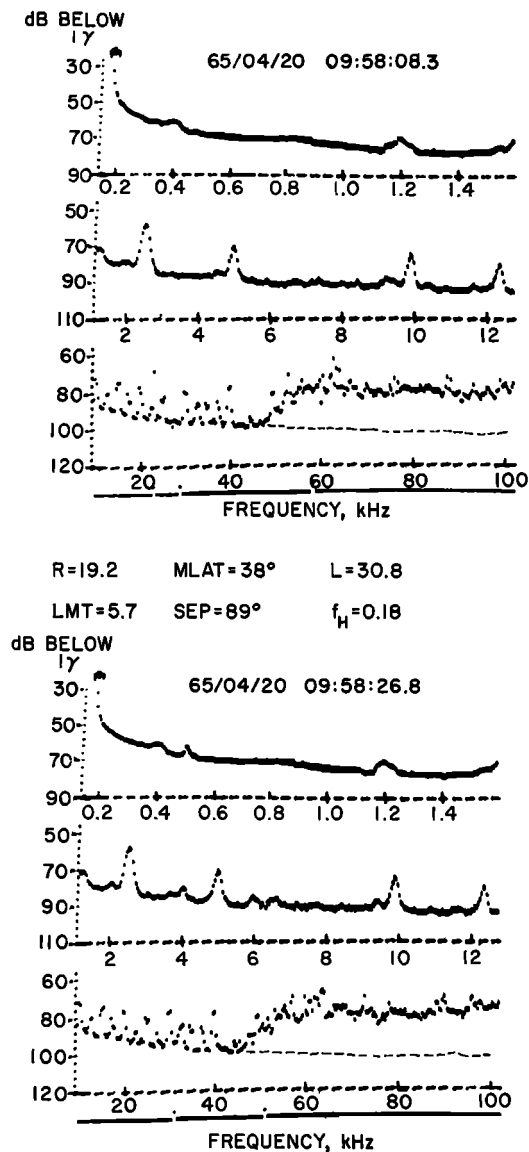


Fig. 2. Two consecutive frames from OGO 1 demonstrating highpass noise with a spectrum extending from 45 kHz to above 100 kHz in the third graph. Except for a slight decrease in low-frequency cutoff from upper to lower frame, the spectrum is relatively consistent between frames. The dashed line in the third graph represents approximate background level of receiver. Other details as in Figure 1.

at least one frame with no detectable noise. The longest duration of a recorded burst is 5.9 hours, the shortest 1 min, and the mean 23 min. The maximum observed power density of a burst is  $10^{-13}$  watt  $m^{-2}$   $Hz^{-1}$  (using free-space conver-

sion values), and the geometric mean of the maximum power densities of all bursts is  $3 \times 10^{-16}$  watt  $\text{m}^{-2}$   $\text{Hz}^{-1}$ . Over the observed bandwidth of approximately 50 kHz, the mean power density is thus  $15 \times 10^{-10}$  watt  $\text{m}^{-2}$ . The mean intensity of whistler-mode noise near the equator is 5 mV at  $L = 5$  [Dunckel and Helliwell, 1969]. For a refractive index of 10, this is equivalent to  $6 \times 10^{-10}$  watt  $\text{m}^{-2}$ . Hence the maximum power in an average highpass noise burst is at least comparable to that of whistler-mode noise. If highpass noise extends to several hundred kilocycles, it may be considerably stronger than whistler-mode noise.

The approximate minimum cutoff of each burst is plotted in the lower part of Figure 3 versus geocentric distance in earth radii. Although the data exhibit scatter, the lower boundary of points shows a tendency of the minimum cutoff to decrease with increasing radial distance. Cutoff frequencies of 40 to 100 kHz appear to be almost equally common from geocentric distances of 4 earth radii out to apogee, whereas values below 40 kHz are common only beyond 10 to 15 earth radii. The lack of points toward the low-frequency side of Figure 3 and the scatter of points elsewhere indicate that the cutoff frequency tends to vary in a semirandom fashion above a lower limit that decreases in frequency as the satellite moves outward, but that becomes constant at  $R > 10$  earth radii. The distribution of cutoff frequencies appearing in the upper part of Figure 3 shows that the most common cutoff frequency is 40 kHz.

#### PATTERNS OF OCCURRENCE

Broadband and highpass noises tend to occur in conjunction with one another. We shall therefore consider the occurrence of both phenomena together in spatial sectors ( $\Delta L = 1$  earth radius,  $\Delta LMT = 2$  hours) by noting the occurrence of highpass or broadband noise during each satellite traversal of a sector. The percentage ratio of traversals on which any noise was observed is plotted in Figure 4. Broadband and highpass noise appear to be mainly nighttime phenomena confined to a region that lies closest to the earth near local midnight. Noise events have never been observed inside the approximate position of the plasmopause, as determined by VLF observations [Dunckel and Helliwell, 1969],

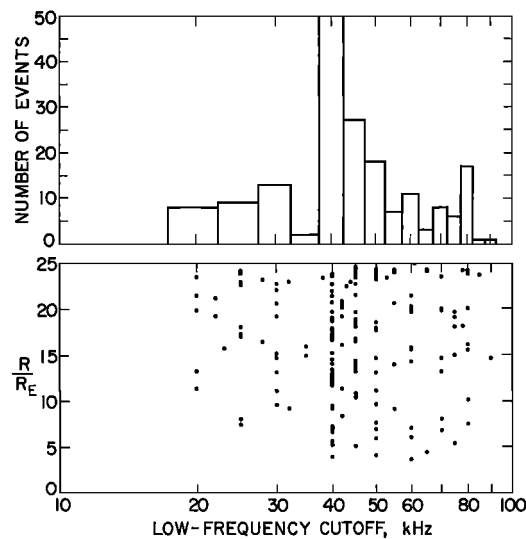


Fig. 3. *Top*: Distribution of minimum cutoff frequency in highpass noise bursts. *Bottom*: Scatter plot of minimum cutoff frequency versus geocentric distance in earth radii. Cutoff appears to occur at random frequencies, but lowest frequencies are common only at large radial distances. Highest frequencies are common at all radial distances greater than 4 earth radii. The most common low-cutoff frequency is 40 kHz.

although events have occurred as close as 1 earth radius in  $L$  value to the plasmopause. Both the overall occurrence pattern and individual events display a marked anti-correlation with the intensity of whistler-mode noise detected by the same experiment [Dunckel and Helliwell, 1969].

Data from  $L > 11$  are incomplete in local time coverage and consequently have not been included in Figure 4. The data available from this outer region indicate that events at large geocentric distances are seen mainly on the nightside. Both types of noise are prevalent out to apogee (a geocentric distance of 24 earth radii) near the dawn and dusk meridians. Comparisons with the OGO 1 observations of Holzer *et al.* [1966] show that bursts occur both inside and outside the mean position of the magnetopause. Most events have been detected at magnetic latitudes from  $20^\circ$  to  $40^\circ$ N.

The percentage of observing time during which these noises occurred has been estimated from 40 hours of data obtained at local mean times between 16 and 22 hours and at  $L > 10$ . Broadband and highpass noises were observed

above the receiver threshold 12% and 27%, respectively, of the total time. Further analysis of the occurrence data is clearly desirable, and both the spatial and magnetic disturbance dependences should be examined.

Comparison of Figure 4 with the contours of median intensity of trapped electron fluxes

( $E \leq 40$  kev) obtained by Injun 3 [Frank *et al.*, 1964] indicates that these LF noises may occur consistently outside the trapping boundary. This interpretation is supported by comparison with fluxes of electrons having energies greater than 40 kev measured on OGO 1 by Rao [1967].

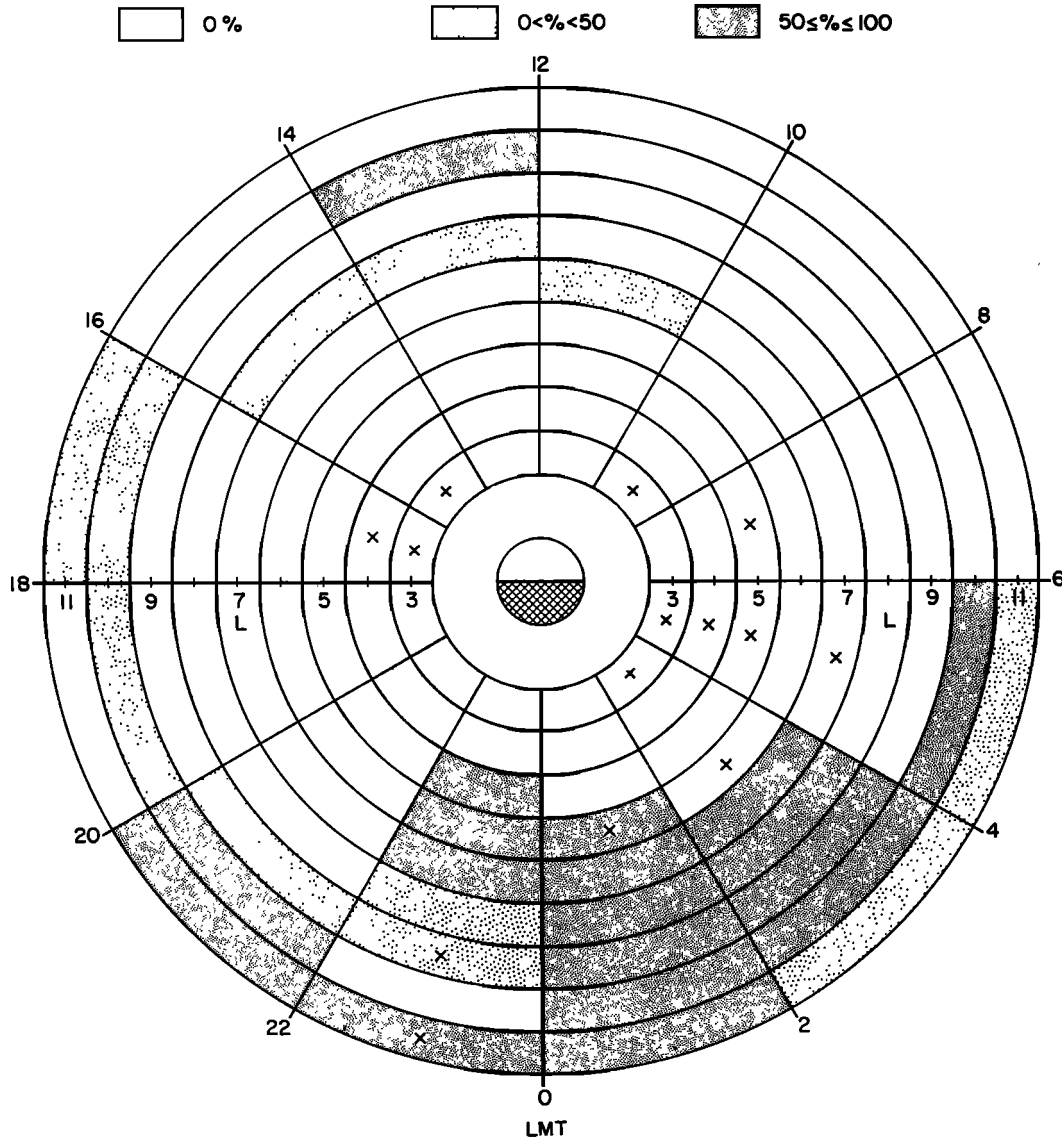


Fig. 4. Occurrence of broadband and highpass noise versus  $L$  in earth radii and local mean time in hours for  $L$  based on Jensen-Cain field. Shading represents ratio of number of passes through each sector containing either highpass noise or broadband noise to total number of passes through that sector. Sectors marked by crosses, for which no data are available, have been assigned the darkest shading appearing on two or more sides. Noises occur predominantly in the dark hemisphere approaching lowest  $L$  shells near the midnight meridian.

*Relation to magnetic activity.* Both broadband and highpass noise events display a close relationship to the auroral electrojet index  $AE$ . This index represents the difference in gammas between the hourly maximum and minimum deviations of the  $H$  trace recorded at any of approximately 10 observatories spaced in longitude around the auroral zone [Davis and Sugiura, 1966; Davis and Wong, 1967]. The close statistical correlation between  $AE$  and 32 highpass and broadband noise events recorded in 1964 is shown in Figure 5. For this presentation values of  $AE$  falling closest to 0,  $\pm 1$ ,  $\pm 2$ , and  $\pm 3$  hours with respect to the time of each event were recorded and the mean was taken for each hour. The geometric mean was employed to reduce the dominance of large values of  $AE$  (however, a plot

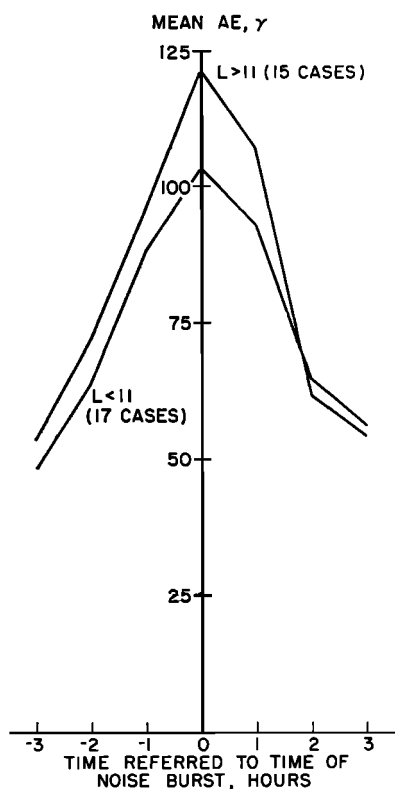


Fig. 5. Variation of the auroral electrojet index  $AE$  with respect to the time of occurrence of 32 broadband and highpass noise events. Mean  $AE$  nearest to time of events (0 hours) shows marked increase over those further removed in time. Little difference appears between data recorded at low  $L$  ( $<11$ ) and high  $L$  ( $>11$ ).

of the arithmetic mean of  $AE$  turned out to have much the same shape). The auroral electrojet index is seen to be highest at the time of the noise burst and significantly lower both before and after the noise burst. Since the data include periods of nearly continuous activity, the curve of Figure 5 is no doubt broader than if only isolated events were included.

Four individual highpass noise events have been compared with geophysical measurements from Byrd Station, Antarctica ( $71^{\circ}\text{S}$  geomagnetic). During these events the satellite was in the northern hemisphere within  $45^{\circ}$  of the geographic longitude of Byrd, at geocentric distances from 18 to 24 earth radii, and at local times from 18 to 20 hours. The commencement of each event on OGO 1 was preceded within 2 min by the onset at Byrd of micropulsations with periods in the range 0.5 to 4 min (the accuracy of these comparisons is limited by the difficulty of establishing the micropulsation onset time to better than 1 min). The commencement of at least one event at the satellite corresponded within 2 min to the onset at Byrd of auroral hiss [Helliwell, 1965] and to an abrupt change in the amplitude and apparent phase of VLF station NPG. One event was followed in 14 min by the commencement of a bay in the Byrd magnetometer records. On the basis of these initial comparisons, it appears that a minute-to-minute correspondence exists between noise events observed at large geocentric distances and geophysical phenomena in the earth's polar regions. This relationship is presently being studied in greater detail.

#### DISCUSSION AND CONCLUSIONS

Broadband and highpass noises appear to be emissions generated in the vicinity of the earth. Their localized region of occurrence and their close relationship to polar geophysical conditions are proof that they are not spurious products of the equipment. For the same reasons, sources that lie outside the earth's environment, such as the sun and Jupiter, are unlikely to cause the observed emissions.

*Origin of broadband noise.* Since part of its observed spectrum lies in a nonpropagating band, broadband noise may well originate in the vicinity of the satellite. In Figure 1, electron gyro- and plasma frequencies of 3 and 10 kHz,

respectively, would produce a nonpropagating band between 3 and 9 kHz under cold plasma conditions [Ratcliffe, 1959]. Since components within this band of frequencies do appear with undiminished intensity, we suspect that broadband noise is generated near the satellite. The generation mechanism may be similar to that of shot noise in a vacuum tube. Consequently, the observed modulation at the spin period of the satellite may be due to the antenna being shielded from the particle source by the satellite body during part of the revolution. Confirmation of this mechanism awaits the outcome of a detailed examination of the relationship between broadband noise intensity and spacecraft orientation.

*Interpretation of highpass noise spectrum.* The low-frequency cutoff of the noise may well represent a propagation cutoff on the path between the source and the receiver. In this case the cutoff frequency should be near the electron plasma frequency. Estimates of local electron density made by Vasyliunas [1968] on the same satellite imply a local plasma frequency about one-fifth of the observed cutoff frequency. Thus this comparison suggests that the cutoff occurs at a distant point where the plasma is more dense than that near the satellite.

*Origin of highpass noise.* One possible source of highpass noise is incoherent synchrotron emission from local electrons. This mechanism would qualitatively account for the observed spectrum of highpass noise, since a cutoff would be expected at a frequency somewhat above the plasma frequency [Vesecky, 1967; Ramaty, 1968]. Using the electron energy distributions given by Frank [1967] in Schwinger's [1949] formulation for synchrotron emission in free space, we obtain a power spectral density tens of orders of magnitude below that observed. Since the presence of the plasma will reduce the radiated power still further, we are forced to reject this hypothesis. Cerenkov radiation, which may occur below the electron plasma and gyrofrequencies or between the electron plasma and upper-hybrid resonance frequencies, cannot reach the satellite under the assumptions of cold plasma theory. The unstable electrostatic waves believed by Perkins [1968] to be generated above the auroral zone are unlikely to produce the high intensities observed by the

magnetic detector without first being converted to electromagnetic waves.

One possibility is that highpass noise represents cyclotron radiation generated close to earth. For the mode that can propagate to the satellite, the wave frequency must be above the plasma frequency and the refractive index is of the order of unity. Hence we can again employ Schwinger's free-space formulation. Using the electron energy distribution employed by Jørgensen [1968] and assuming confinement of the radiation along fieldlines, we obtain a power spectral density about 4 orders of magnitude below that observed.

A feature of this model is that it accounts for the approximate magnitude of the cutoff frequency. Generation at  $f_H$  from a region in space will occur as long as  $f_H$  is greater than the plasma frequency. Since  $f_H$  decreases relatively rapidly with increasing altitude, a cutoff will occur at the frequency at which  $f_H$  equals the plasma frequency. Reasonable plasma frequencies of about 40 kHz at geocentric distances of about 3 earth radii near auroral field lines are thus implied by the cutoff measurements.

The data are being further examined and are being compared both with ground data and with data from related experiments on OGO 1. These studies should help to identify the sources of both broadband and highpass noise.

*Acknowledgments.* The participation of W. E. Blair and N. D. Schlosser in the analysis is gratefully acknowledged. We thank D. L. Carpenter both for his helpful suggestions concerning the analysis of the data and for his comments on the manuscript. We appreciate the efforts of the many participants in the OGO program who contributed significantly to the success of this experiment. This research was supported by the National Aeronautics and Space Administration under contracts NAS 5-2131 and NGR 05-020-288, and under grant NSG 174-SC/05-020-008.

#### REFERENCES

- Benediktov, E. A., G. G. Getmantsev, N. A. Mitjakov, V. O. Rapoport, J. A. Sazonov, and A. F. Tarasov, Intensity measurements of radiation at frequencies 725 and 1525 Kc, by means of the receiver on the satellite 'Electron-2,' *Space Res.*, **6**, 110, 1969.
- Davis, T. N., and M. Sugiura, Auroral electrojet activity index  $AE$  and its universal time variations, *J. Geophys. Res.*, **71**, 785, 1966.
- Davis, T. N., and Y. S. Wong, Hourly values of the auroral electrojet activity index  $AE$  for



- 1964, *Rept. UAG R-198*, Univ. Alaska, College, Alaska, 1967.
- Dunckel, N., and R. A. Helliwell, Whistler-mode emissions on the OGO 1 satellite, *J. Geophys. Res.*, **74**(26), 6371, 1969.
- Frank, L. A., Initial observations of low-energy electrons in the earth's magnetosphere with OGO 3, *J. Geophys. Res.*, **72**, 185, 1967.
- Frank, L. A., J. A. Van Allen, and J. D. Craven, Large diurnal variations of geomagnetically trapped and of precipitated electrons observed at low altitudes, *J. Geophys. Res.*, **69**, 3155, 1964.
- Fritz, R. B., E. R. Schiffmacher, and J. K. Hargreaves, Response of ionospheric and exospheric electron contents to a partial solar eclipse, *J. Geophys. Res.*, **73**, 4994, 1968.
- Haddock, F. T., Low-frequency radioastronomy, in *Space Astronomy 1958-1964*, NASA SP-91, p. 49, Scientific and Technical Information Division, National Aeronautics and Space Administration, Washington, D. C., 1966.
- Hartz, T. R., Satellite observations of ionospheric radio noise, *Progress in Radio Science 1963-1966*, Proc. 15th General Assembly URSI, Munich, September 5-15, 1966, p. 1109, 1967.
- Hartz, T. R., Radio noise levels within and above the ionosphere, *Proc. IEEE*, **57**, 1042, 1969.
- Harvey, C. C., Results from the UK-2 satellite, *Ann. Astrophys.*, **28**, 248, 1965.
- Harvey, C. C., Radio emission from geomagnetically trapped particles, *Nature*, **217**, 50, 1968.
- Helliwell, R. A., *Whistlers and Related Ionospheric Phenomena*, Stanford University Press, Stanford, California, 1965.
- Heyborne, R. L., Observations of whistler-mode signals in the OGO satellites from VLF ground station transmitters, *Tech. Rep. 3415/3418-1*, Stanford Electronics Lab., Stanford University, Stanford, California (Ph.D. thesis), 1966.
- Holzer, R. E., M. G. McLeod, and E. J. Smith, Preliminary results from the OGO 1 search-coil magnetometer: Boundary positions and magnetic noise spectra, *J. Geophys. Res.*, **71**, 1481, 1966.
- Huguenin, G. R., and M. D. Papagiannis, Spaceborne observations of radio noise from 0.7 to 7.0 MHz and their dependence on the terrestrial environment, *Ann. Astrophys.*, **28**, 239, 1965.
- Jørgensen, T. S., Interpretation of auroral hiss measured on OGO 2 and at Byrd Station in terms of incoherent Cerenkov radiation, *J. Geophys. Res.*, **73**, 1055, 1968.
- Perkins, F. W., Plasma-wave instabilities in the ionosphere over the aurora, *J. Geophys. Res.*, **73**, 6631, 1968.
- Ramaty, Reuven, Determination of the coronal magnetic field and the radio-emitting electron energy from a type 4 solar radio burst, *Solar Phys.*, **5**, 531, 1968.
- Rao, C. S. R., Study of the temporal variations of 40-keV electrons in the magnetosphere during and after the magnetic storm on April 18, 1965, *Rep. 67-16*, Dept. Phys. Astron., Univ. Iowa, Iowa City, Iowa, May 1967.
- Ratcliffe, J. A., *The Magneto-Ionic Theory and Its Applications to the Ionosphere*, Cambridge University Press, Cambridge, 1959.
- Schwinger, J., On the classical radiation from accelerated electrons, *Phys. Rev.*, **75**, 1912, 1949.
- Slysh, V. I., Measurements of kilometer cosmic radio waves in interplanetary space, *Cosmic Res.*, **4**, 794, 1966.
- Slysh, V. I., Observation of type-III radiobursts on AIS 'Venera-2,' *Astron. Zh. SSSR*, **44**, 487, 1967; English translation appears as *NASA Rep. CR-86633*, 29 June 1967a.
- Slysh, V. I., Long-wavelength solar radio emission observed by the lunar satellites Luna 11 and Luna 12, *Cosmic Res.*, **5**, 759, 1967b.
- Vasyliunas, M. V., A survey of low-energy electrons in the evening sector of the magnetosphere with OGO 1 and OGO 3, *J. Geophys. Res.*, **73**, 2839, 1968.
- Vesceky, John F., Radio frequency synchrotron radiation from electrons trapped in the earth's magnetic field, *Tech. Rep. 3606-2*, Stanford Electronics Lab., Stanford University, Stanford, California, August 1967.

(Received September 8, 1969;  
revised December 2, 1969.)